

MHD Casson Fluid Flow through a Parallel Plate

Md. Afikuzzaman and Md. Mahmud Alam*

Mathematics Discipline

Science, Engineering and Technology School, Khulna University,
Khulna-9208, Bangladesh

Abstract

Free convection and mass transfer Casson fluid flow through a parallel plate with uniform magnetic field is investigated. The uniform magnetic field is applied perpendicular to the plates and the fluid motion is subjected to a uniform suction and injection. The upper plate is moving and the lower plate is stationary. The momentum, energy and concentration equations have been solved by explicit finite difference method. The stability conditions and convergence analysis of the explicit finite difference scheme are established for finding the restriction of the values of various parameters to obtain converse solutions. The influence of various interesting parameters on the flow has been analyzed and discussed through graph in details. The values of Shear Stress, Nusselt number and Sherwood number for both moving and stationary plates for different physical parameters are also discussed in the graphical form.

Keywords: MHD; Explicit finite difference techniques; Hall current; Viscous dissipation; Thermal diffusion

1. Introduction

The Analysis of non-Newtonian Casson fluid flow has been the focus of extensive research by various scientists due to its importance in many devices such as magnetohydrodynamic (MHD), power generators, MHD pumps, aerodynamics heating, polymer extrusion, petroleum industry, pharmaceutical process, purification of crude oil, fluid droplet sprays, metal forming, wire and glass fiber drawing and several others. The fluid flow of Casson fluid by means of Couette motion is a classical fluid mechanics problem. The industrial applications of non-Newtonian Casson fluid flow are increasing day by day. Among the many industrial non-Newtonian fluids some fluids behave like elastic solids, and for those fluids, a yield shear stress exists in the

constitutive equations. The configuration is a good approximation of some practical situations such as heat exchangers, flow meters and pipes that connects system components. The non-linear Casson's constitutive equation has been found to describe accurately the flow curves of suspensions of pigments in lithographic varnishes used for preparation of printing inks and silicon suspensions. Tao [1] studied the Magnetohydrodynamic effect on the formation of Couette flow. Soundalgekar et al. [2] considered Hall and Ion-slip effects in MHD Couette flow with heat transfer. Transient effects in natural convection cooling of vertical plates were showed by Joshi [3]. Das and Batra [4] investigated Secondary flow of a Casson fluid in a slightly curved tube. Dash et al. [5] proposed a theory

on hydromagnetic flow between two horizontal porous plates into account with finite difference analysis. Attia and Ahmed [6] analyzed Hydrodynamic impulsive Lid driven flow and heat transfer of a Casson fluid. Such type of flow can be used in Civil engineering point of view. For bridge construction, the flow between two piers can be measured. Attia [7] gave the effect of variable properties on the unsteady Couette flow with heat transfer considering the hall effect which is very much related to Casson fluid. Haque and Alam [8] derived MHD heat and mass transfer flow of micropolar fluid. Krisnendu Bhattacharyya [9] showed MHD stagnation point flow of Casson fluid and heat transfer over a stretching sheet with thermal radiation. Kabir and Alam [10] investigated Unsteady Casson fluid flow through a parallel plate with hall current, joule heating and viscous dissipation.

Hence our aim is to extend the work of Kabir and Alam [10] in the case of mass transfer. The system is considered as such that the upper plate is moving with a uniform velocity while the lower plate is fixed. A constant pressure gradient act on the flow and uniform magnetic field is applied perpendicular to the plates. The proposed model has been transformed into nonlinear coupled partial differential equations by usual transformations. The governing momentum, energy and concentration equations are solved numerically in case of one dimension flow and explicit finite difference method has been used to calculate the results and convergence analysis. Finally, the values of Shear Stress, Nusselt number and Sherwood number for both moving and stationary plates for different physical parameters are illustrated in the form of graphs.

2. Mathematical Formulations

The fluid is assumed viscous, laminar and incompressible flows between two infinite horizontal plates located at $y = \pm h$ planes and extended from $x = -\infty$ to ∞ and from $z = -\infty$ to ∞ . The lower plate is stationary while the upper plate moves with a uniform velocity U_0 . The upper and lower plates are kept at two constants temperature T_2 and T_1 respectively with $T_2 > T_1$ and concentration C_2 and C_1 with $C_2 > C_1$. The fluid is acted

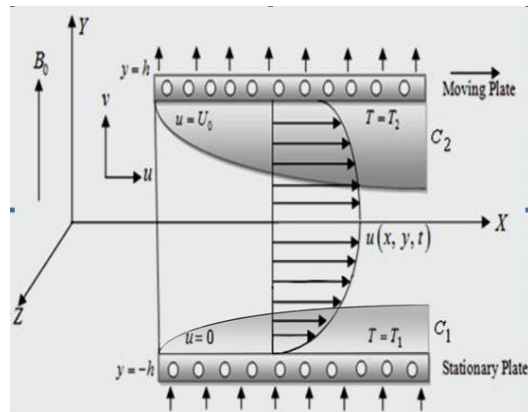


Fig.1. Geometrical Configuration of the flow

upon by an exponentially decaying pressure gradient $-\frac{\partial p}{\partial x}$ in the x direction and a uniform suction from above and injection from below which are applied at $t = 0$.

A uniform magnetic field is applied in the positive y -direction and is assumed undistributed as the induced magnetic field is neglected by assuming a very small magnetic Reynolds number. The Hall effects are taken into consideration and consequently a z -component for the velocity is expected to arise. The uniform suction implies that the y -component of the velocity v_0 is constant. Thus the fluid velocity vector is given by;

$$v = u\mathbf{i} + v_o\mathbf{j} + w\mathbf{k}$$

By using generalized Ohm's law, the MHD free convection and mass transfer fluid flows are governed by the following equations.

Continuity equation: $\frac{\partial v}{\partial y} = 0$ (1)

which gives $v = -v_o$ (constant)

Momentum equations in x and z axis:

$$\frac{\partial u}{\partial t} - v_o \frac{\partial u}{\partial y} = -\frac{1}{\rho} \frac{\partial p}{\partial x} + g\beta(T - T_1) + g\beta^*(C - C_1)$$

$$+ \frac{1}{\rho} \frac{\partial}{\partial y} \left(\mu \frac{\partial u}{\partial y} \right) - \frac{\sigma B_o^2}{\rho(1+m^2)} (u + mw) - \frac{v}{k} u$$

$$\frac{\partial w}{\partial t} - v_o \frac{\partial w}{\partial y} = \frac{1}{\rho} \frac{\partial}{\partial y} \left(\mu \frac{\partial w}{\partial y} \right) - \frac{\sigma B_o^2}{\rho(1+m^2)} (w - mu) - \frac{v}{k} w$$

(2)

(3)

Energy equation:

$$\rho C_p \frac{\partial T}{\partial t} - \rho C_p v_o \frac{\partial T}{\partial y} = k \frac{\partial^2 T}{\partial y^2}$$

$$+ \mu \left[\left(\frac{\partial u}{\partial y} \right)^2 + \left(\frac{\partial w}{\partial y} \right)^2 \right] + \frac{\sigma B_o^2}{1+m^2} (u^2 + w^2)$$

(4)

Concentration equation:

$$\frac{\partial C}{\partial t} - v_o \frac{\partial C}{\partial y} = D_m \frac{\partial^2 C}{\partial y^2} + \frac{D_m k_t}{T_m} \frac{\partial^2 T}{\partial y^2}$$

(5)

The corresponding initial and boundary conditions are;

$$t = 0, u = 0, w = 0, T = T_1, C = C_1$$

,everywhere

$$t \geq 0, u = 0, w = 0, T = T_1, C = C_1 \text{ at } y = -h$$

$$y = -h$$

$$u = U_o, w = 0, T = T_2, C = C_2 \text{ at } y = h$$

The non-dimensional variables that have been used in the governing equations are;

$$\bar{x} = \frac{xU_o}{v}, \bar{y} = \frac{yU_o}{v}, \bar{t} = \frac{tU_o^2}{v}, \bar{u} = \frac{u}{U_o},$$

$$\bar{w} = \frac{w}{U_o}, \bar{v} = \frac{v}{U_o}, \bar{p} = \frac{p}{\rho U_o^2}, \bar{C} = \frac{C - C_1}{C_2 - C_1},$$

$$\theta = \frac{T - T_1}{T_2 - T_1}, \bar{\mu} = \frac{\mu}{K_c^2}$$

Using these above dimensionless variable the following dimensionless equations have been obtained as;

$$\frac{\partial u}{\partial t} - S \frac{\partial u}{\partial y} = -\alpha e^{-dt} + \frac{\partial^2 u}{\partial y^2} + G_r \theta + G_m C$$

$$- \frac{M}{(1+m^2)} (u + mw) - \gamma u$$

(6)

$$\frac{\partial w}{\partial t} - S \frac{\partial w}{\partial y} = \frac{\partial^2 w}{\partial y^2} - \frac{M}{(1+m^2)} (w - mu) - \gamma w$$

(7)

$$\frac{\partial \theta}{\partial t} - S \frac{\partial \theta}{\partial y} = \frac{1}{P_r} \frac{\partial^2 \theta}{\partial y^2} + \frac{E_c M}{(1+m^2)} (u^2 + w^2)$$

$$+ E_c \left[\left(\frac{\partial u}{\partial y} \right)^2 + \left(\frac{\partial w}{\partial y} \right)^2 \right]$$

(8)

$$\frac{\partial C}{\partial t} - S \frac{\partial C}{\partial y} = \frac{1}{S_c} \frac{\partial^2 C}{\partial y^2} + S_r \frac{\partial^2 \theta}{\partial y^2}$$

(9)

where α is the constant pressure gradient $\left(\frac{dp}{dx} \right)$ and d is the decaying parameter.

The corresponding initial and boundary conditions are;

$$t = 0, u = 0, w = 0, T = 0, C = 0, \text{ everywhere}$$

$$t \geq 0, u = 0, w = 0, T = 0, C = 0 \text{ at } y = -1$$

$$u = 1, w = 0, T = 1, C = 1 \text{ at } y = 1$$

The non-dimensional quantities are;

Suction parameter $S = \frac{\nu_o}{U_o}$, Magnetic

parameter $M = \frac{\sigma B_o^2 \nu}{\rho U_o^2}$, Permeability of the

porous medium $\gamma = \frac{\nu^2}{k U_o^2}$, Eckert number

$E_c = \frac{U_o^2}{C_p (T_2 - T_1)}$, Prandtl number

$P_r = \frac{\rho C_p \nu}{k}$, Schmidt number $S_c = \frac{\nu}{D_m}$,

Soret number $S_r = \frac{D_m K_t (T_2 - T_1)}{\nu T_m (C_2 - C_1)}$,

Grashoff number $G_r = \frac{g \beta (T_2 - T_1) \nu}{U_o^3}$,

Modified Grashoff number $G_m = \frac{g \beta^* (C_2 - C_1) \nu}{U_o^3}$

From the velocity field, the effects of various parameters on Shear Stress have been studied. The dimensionless Shear stress for moving wall is given by;

$$\tau_{w1} = \left[\left[\left(\left(\frac{\partial u}{\partial y} \right)^2 + \left(\frac{\partial w}{\partial y} \right)^2 \right)^{\frac{1}{4}} + \frac{\tau_D^{1/2}}{\left(\left(\frac{\partial u}{\partial y} \right)^2 + \left(\frac{\partial w}{\partial y} \right)^2 \right)^{\frac{1}{4}}} \right]^2 \right]_{y=-1}$$

The dimensionless Shear stress for stationary wall is given by;

$$\tau_{w2} = \left[\left[\left(\left(\frac{\partial u}{\partial y} \right)^2 + \left(\frac{\partial w}{\partial y} \right)^2 \right)^{\frac{1}{4}} + \frac{\tau_D^{1/2}}{\left(\left(\frac{\partial u}{\partial y} \right)^2 + \left(\frac{\partial w}{\partial y} \right)^2 \right)^{\frac{1}{4}}} \right]^2 \right]_{y=1}$$

From the temperature field, the effects of various parameters on Nusselt number have been described. The dimensionless Nusselt number at the moving and stationary wall respectively is given by;

$$Nu_1 = \frac{\left(2 \frac{\partial T}{\partial y} \right)_{y=1}}{T_m - 1}, Nu_2 = \frac{\left(2 \frac{\partial T}{\partial y} \right)_{y=-1}}{-T_m}$$

The dimensionless Sherwood numbers at the moving wall is given by;

$$Cu_1 = \frac{\left(2 \frac{\partial C}{\partial y} \right)_{y=1}}{C_m - 1},$$

The dimensionless Sherwood numbers at the stationary wall is given by;

$$Cu_2 = \frac{\left(2 \frac{\partial C}{\partial y} \right)_{y=-1}}{-C_m}$$

where T_m and C_m are the dimensionless mean fluid temperature and dimensionless mean fluid concentration respectively and are defined as

$$T_m = \frac{2 \int_{-1}^1 u T dy}{\int_{-1}^1 u dy} \quad \text{and} \quad C_m = \frac{2 \int_{-1}^1 u C dy}{\int_{-1}^1 u dy}$$

respectively.

3. Numerical Analysis

For simplicity the explicit finite difference method has been used to solve equations (6-9) subject to the initial and boundary conditions. In this case the region within the boundary layer is divided by some perpendicular line of Y -axis, where Y -axis is normal to the medium as shown in the Fig.2.

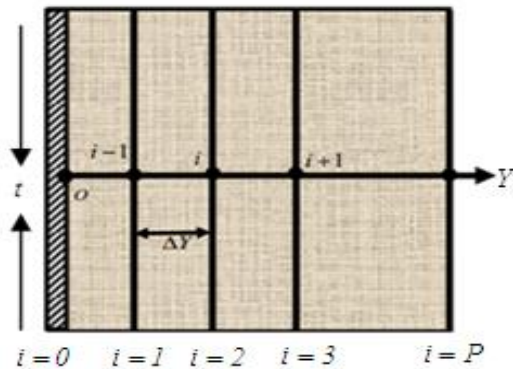


Fig.2. Finite difference grid space.

It is assumed that the maximum length of the boundary layer is $Y_{\max} = 2$ i.e. Y varies from -1 to $+1$ and the number of grid spacing in Y direction is $P=100$. Hence the constant mesh size along Y -axis becomes $\Delta Y = 0.02 (-1 \leq Y \leq 1)$ with smaller time step $\Delta t = 0.0001$.

Let $U^{n+1}, W^{n+1}, \theta^{n+1}$ and C^{n+1} denote the values U^n, W^n, θ^n and C^n at the end of a time step respectively. Using the explicit finite difference method the system of partial differential equations (6-9) are obtained difference equations as;

$$\frac{U_i^{n+1} - U_i^n}{\Delta t} - S \frac{U_{i+1}^n - U_i^n}{\Delta Y} = -\alpha e^{-dt} + \frac{U_{i+1}^n - 2U_i^n + U_{i-1}^n}{\Delta Y^2} + G_r \theta_i^n + G_m C_i^n -$$

$$\frac{M}{(1+m^2)} \left(U_i^n + mW_i^n \right) - \gamma U_i^n \quad (10)$$

$$\frac{W_i^{n+1} - W_i^n}{\Delta t} - S \frac{W_{i+1}^n - W_i^n}{\Delta Y} = \frac{W_{i+1}^n - 2W_i^n + W_{i-1}^n}{\Delta Y^2} - \frac{M}{(1+m^2)} \left(W_i^n - mU_i^n \right) - \gamma W_i^n \quad (11)$$

$$\frac{\theta_i^{n+1} - \theta_i^n}{\Delta t} - S \frac{\theta_{i+1}^n - \theta_i^n}{\Delta Y} = \frac{1}{P_r} \left[\frac{\theta_{i+1}^n - 2\theta_i^n + \theta_{i-1}^n}{\Delta Y^2} \right] + E_c \left[\left(\frac{U_{i+1}^n - U_i^n}{\Delta Y} \right)^2 + \left(\frac{W_{i+1}^n - W_i^n}{\Delta Y} \right)^2 \right] + \frac{E_c M}{(1+m^2)} \left[\left(U_i^n \right)^2 + \left(W_i^n \right)^2 \right] \quad (12)$$

$$\frac{C_i^{n+1} - C_i^n}{\Delta t} - S \frac{C_{i+1}^n - C_i^n}{\Delta Y} = \frac{1}{S_c} \frac{W_{i+1}^n - 2W_i^n + W_{i-1}^n}{\Delta Y^2} + S_r \frac{\theta_{i+1}^n - 2\theta_i^n + \theta_{i-1}^n}{\Delta Y^2} \quad (13)$$

and the initial and boundary conditions with the finite difference scheme are

$$\begin{aligned} t \geq 0, \quad U_L^n = 0, W_L^n = 0, \theta_L^n = 0, C_L^n = 0 \text{ everywhere} \\ t \geq 0, \quad U_L^n = 0, W_L^n = 0, \theta_L^n = 0, C_L^n = 0 \text{ where } L = -1 \\ U_L^n = 1, W_L^n = 0, \theta_L^n = 1, C_L^n = 1 \text{ where } L = 1 \end{aligned}$$

The numerical values of Shear stresses and Sherwood number for both moving plate and stationary plate have been evaluated by five-point approximation formula. Also the numerical values of Nusselt number for two plates have been evaluated by using Five-point approximation formula and Trapezoidal rule. The stability conditions of the method are:

$$\frac{2\Delta t}{(\Delta Y)^2} + \frac{M\Delta t}{2(1+m^2)} + \frac{\gamma\Delta t}{2} + \frac{S\Delta t}{\Delta Y} \leq 1,$$

$$\frac{2\Delta t}{P_r(\Delta Y)^2} + S \frac{\Delta t}{\Delta Y} \leq 1, S \frac{\Delta t}{\Delta Y} - \frac{4\Delta t}{S_c(\Delta Y)^2} \leq 1,$$

and the convergence criteria $S_c \geq 0.60$, $P_r \geq 0.51$, (details are not shown for brevity).

4. Results and Discussion

In order to investigate the physical significance of the problem, the numerical values of Shear Stress, Nusselt number and Sherwood number have been computed for different values of various parameters. To obtain the steady state solutions, the computations have been carried out up to dimensionless time $t = 0$ to $t = 20$. It is seen that, the numerical values of U, W, θ and C show little changes after $t = 5$. Hence at $t = 5$, the solutions of all variables are steady state solutions. The Shear stress, Nusselt number and Sherwood number for both moving and stationary plates have been illustrated in Figs. 3-20.

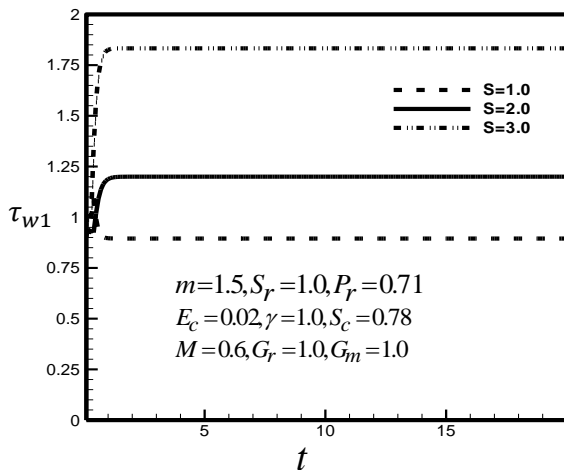


Fig.3. Shear Stress at moving plate for different values of S .

The Shear Stress for both moving and stationary plates for different values of Suction parameter (S) has been presented in Figs. 3-4 respectively. It is observed that Shear Stress increases in the moving plate with the increase of S , where decreases in the stationary plate with increase of S .

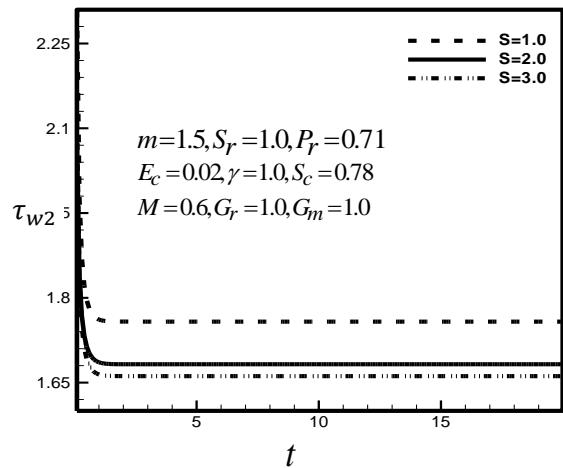


Fig.4. Shear Stress at stationary plate for different values of S .

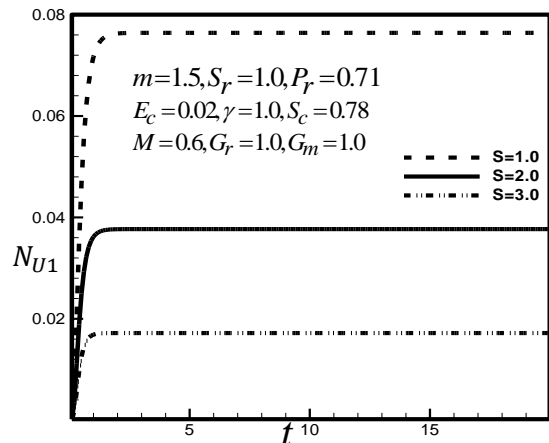


Fig.5. Nusselt number at moving plate for Different values of S .

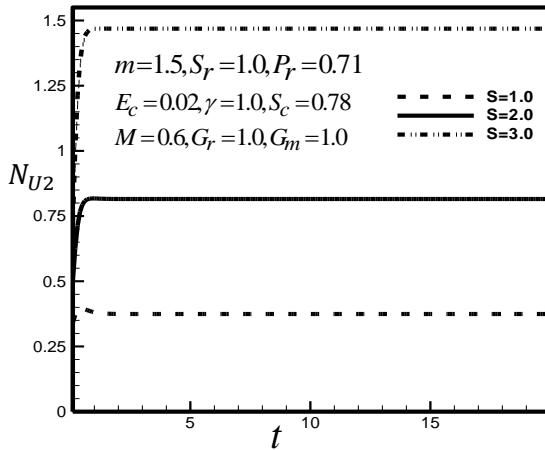


Fig.6. Nusselt number at stationary plate for different values of S .

The effect of Suction parameter (S) on Nusselt number and Sherwood number both at moving and stationary plates are illustrated in Figs.5-8. It is clear that Nusselt number decreases in the upper plate but increases in the lower plate with the increase of S . It is observed, there is an increasing and minor decreasing effect of Sherwood number for two plates at the rise of S . Such types of behavior have been occurred due to moving and stationary plates.

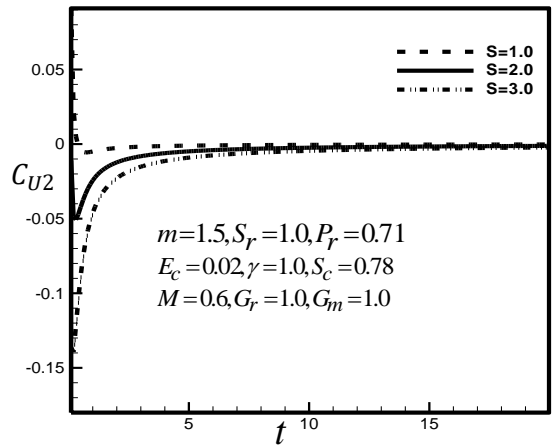


Fig.8. Sherwood number at stationary plate for different values of S .

The influence of Permeability of the porous medium (γ) on Shear stress and Nusselt number both at moving and stationary plates are illustrated in Figs. 9-12. It is observed that Shear stress decreases in the moving plate but increases in the lower plate with the increase of γ . It is also shown from the figure Nusselt number decreases for both moving and stationary plate with the increase of γ .

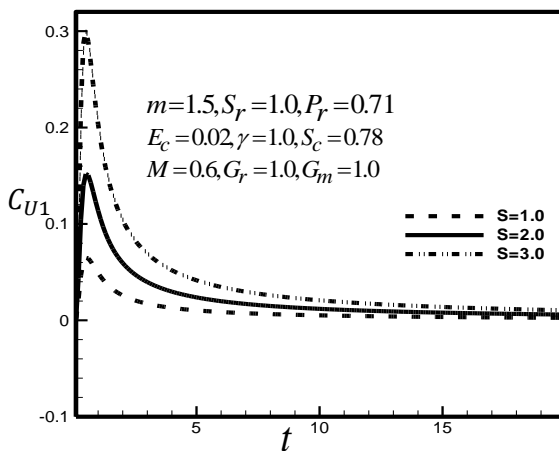


Fig.7. Sherwood number at moving plate for different values of S .

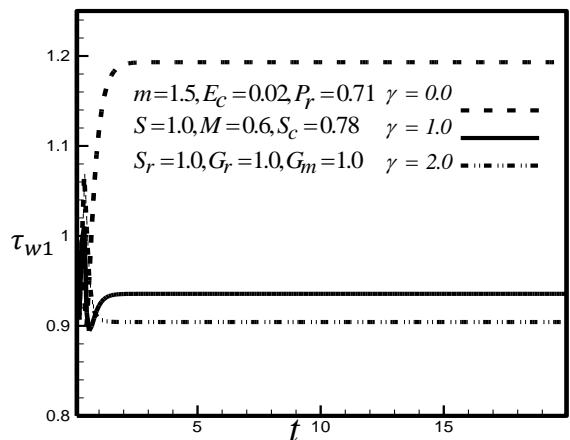


Fig.9. Shear Stress at moving plate for different values of γ

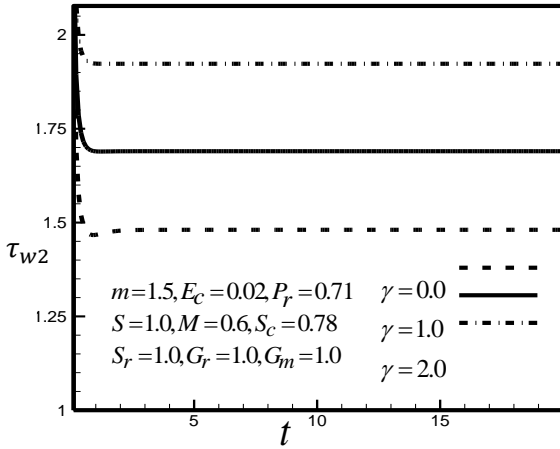


Fig.10. Shear Stress at stationary plate for different values of γ

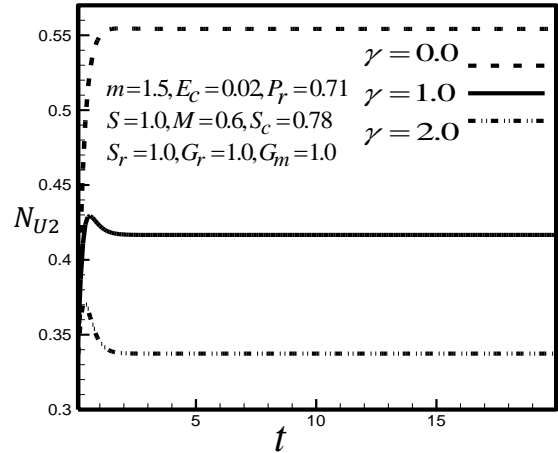


Fig.12. Nusselt number at stationary plate for different values of γ

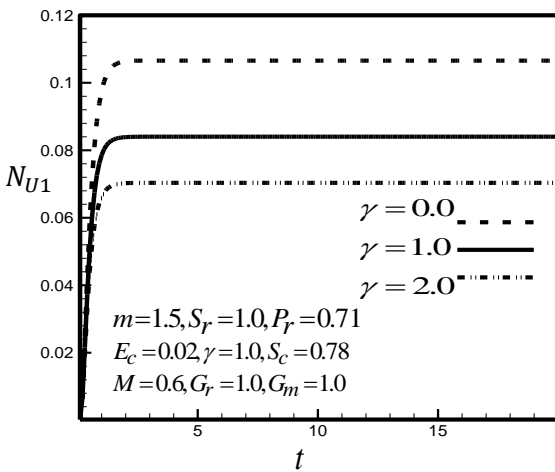


Fig.11. Nusselt number at moving plate for different values of γ

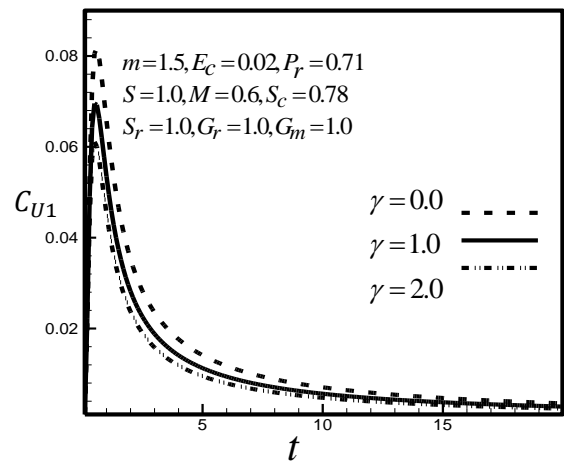


Fig.13. Sherwood number at moving plate for different values of γ

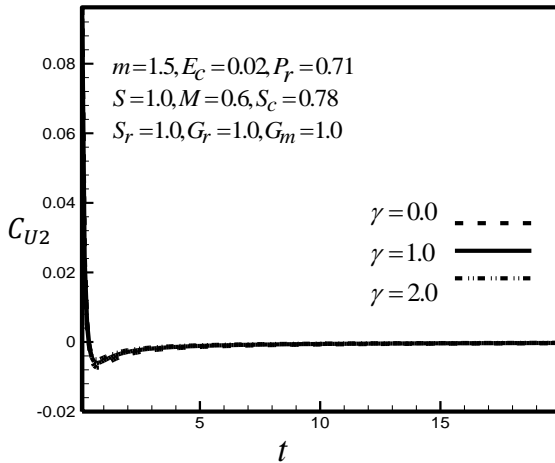


Fig.14. Sherwood number at stationary plate for different values of γ

The effects of γ on Sherwood number has been presented in Fig.13-14 respectively. It is analyzed that Sherwood number decreases in the moving plate but in the stationary plate it has a slightly increasing effect. The decreasing effects are occurred because boundary layer thickness increases due to enhancing γ

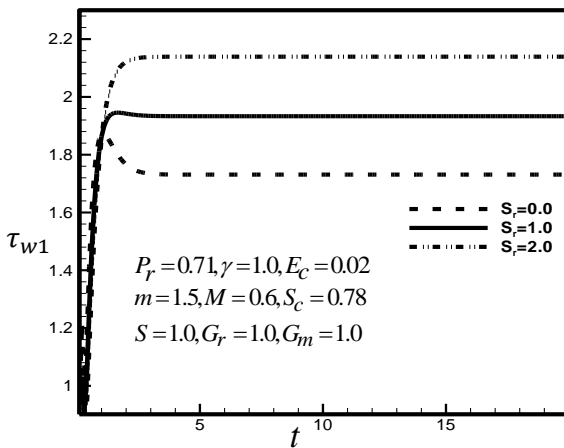


Fig.15. Shear stress at moving plate for different values of S_r

The influence of Soret number (S_r) on Shear stress both moving and stationary plate have been described in the Figs. 15-16 It is shown that Shear stress increases in the both plate with the increase of S_r .

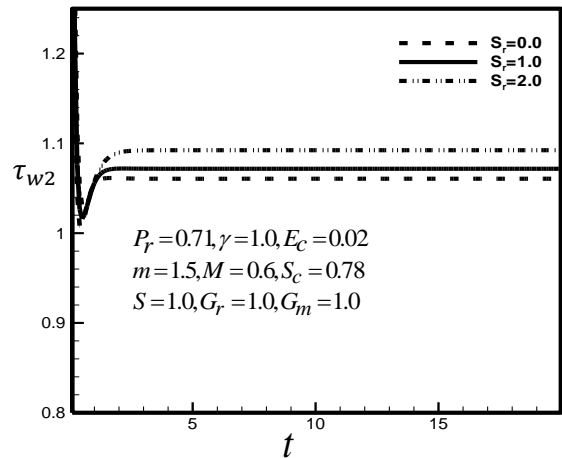


Fig.16. Shear stress at stationary plate for different values of S_r

The influence of Soret number (S_r) on Nusselt number have been described in 17-18. It is observed that Nusselt number have increased in the both plate but in stationary plate it has a minor increasing effect with increase of soret number.

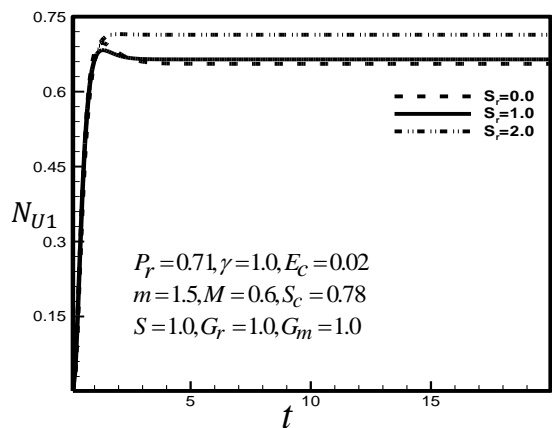


Fig.17. Nusselt number at moving plate for different values of S_r

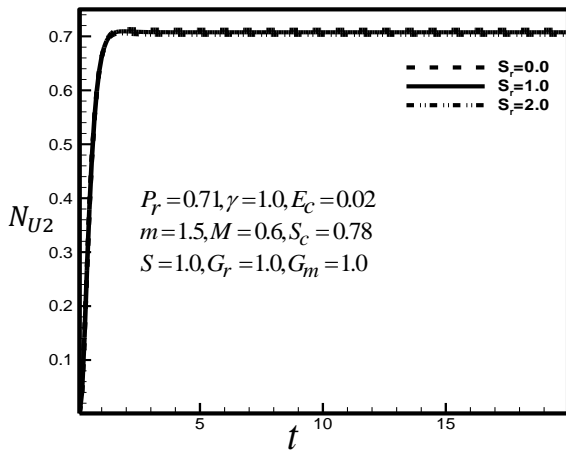


Fig.18. Nusselt number at stationary plate for different values of S_r

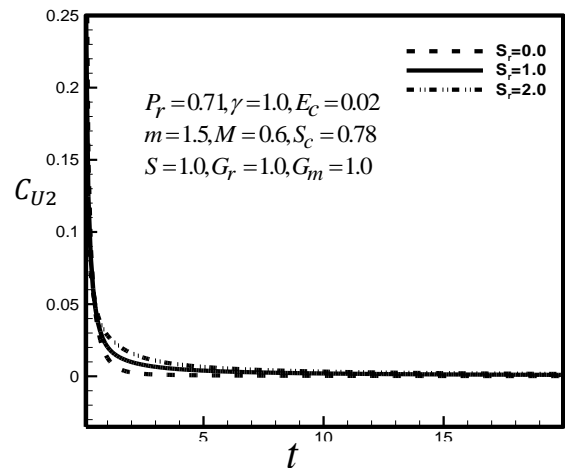


Fig.20. Sherwood number at stationary plate for different values of S_r

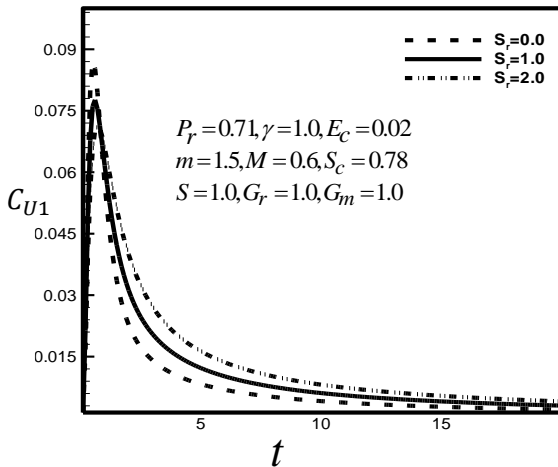


Fig.19. Sherwood number at moving plate for different values of S_r

The effects of Soret number (S_r) on Sherwood number both moving and stationary plate has been described in the Figs. 19-20. It is shown that Sherwood number increases in the both plate with the increase of S_r . Thermal diffusion ratio is the main cause for such type of increasing behaviors.

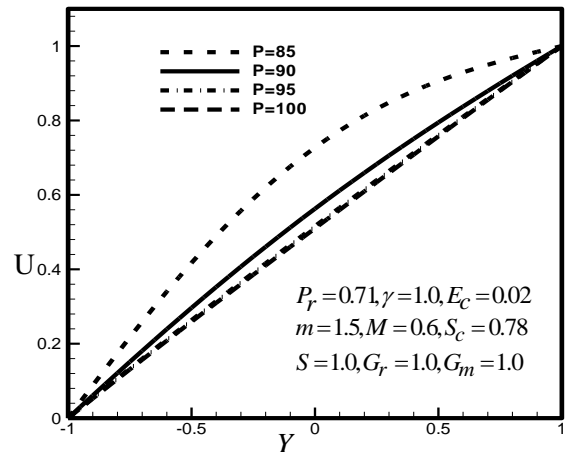


Fig.21. Grid validation for different values of grid space P

5. Conclusions

Casson Fluid flow through a parallel plate under the action of mass transfer by using implicit finite difference method has been taken into consideration. The physical properties are graphically discussed for different values of corresponding parameters. Some important findings of this study are given below:

- 5.1 The Shear stress increases both moving and stationary plate with the increasing S_r .
- 5.2 The Shear stress increases in the moving plate but decreases in the lower plate with the increase of S while it decreases in the moving plate but increase in stationary plate with increase of γ .
- 5.3 The Nusselt number decreases in the both plates with the increase of γ and it decreases in the moving plate but increases in the stationary plate with the increase of S .
- 5.4 The Sherwood number decreases in the moving plate but increases in the lower plate with the increase of γ while it increases in the moving plate but decrease in stationary plate with increase of S .

6. Nomenclature

S	Suction parameter
M	Magnetic parameter
E_c	Eckert number
γ	Permeability of the porous medium
P_r	Prandtl number
S_c	Schmidt number
m	Hall Parameter
S_r	Soret number
G_r	Grashoff number
D_m	Coefficient of mass diffusivity

G_m	Modified Grashoff number
K_t	Thermal diffusion ratio
t	Time
T_m	Mean fluid temperature
u	Velocity component in x -direction
C_m	Mean fluid concentration
v	Velocity component in y -direction
β	Thermal expansion coefficient
w	Velocity component in z -direction
β^*	Concentration expansion coefficient
T	Temperature
P	Fluid pressure
ρ	Density of the fluid
g	Acceleration due to gravity
μ	Apparent viscosity
C_p	Specific heat
ν	Coefficient of kinematic viscosity
k	Thermal conductivity

7. Acknowledgment

This work is financed and supported by National Science and Technology under Ministry of Science and Technology, Government of the People's Republic of Bangladesh.

8. References

- [1] Toa, I.N., Magneto hydrodynamic Effect on the Formulation of Couette flow, Journal of Aerospace Science, Vol. 27, pp. 334-347, 1960.
- [2] Soundalgekar, V.M., Vighnesam, N.V. and Takhar, H.S., Hall and Ion-slip Effects in MHD Couette Flow with Heat Transfer, IEEE Transactions on

- Plasma Science, Vol. 7, No. 3, pp.178-182, 1979.
- [3] Joshi, H.M., Transistant Effects in Natural Convection Cooling of Vertical Plates, Internationa Communications in Heat and Mass Transfer, Vol. 15, pp. 227-238, 1988.
- [4] Das and Batra, R.L., Secondary Flow of a Casson Fluid in a Slightly Curved Tube, Journal of International Nonlinear mechanics, Vol. 28, No. 5, pp. 567-577, 1993.
- [5] Dash, G.C., Panda, Jayaprakash, Das, S.S., Finite Difference Analysis of Hydromagnetic Flow and Heat Transfer of an Elastic Viscous Fluid between Two Horizontal Porous Plate, AMSE Journal, Vol. 73, No. 1-2, 2004.
- [6] Attia H.A. and Sayed-Ahmed, M.E., Hydrodynamic Impulsive Lid Driven Flow and Heat Transfer of a Casson Fluid, Tamakang Journal of Science and Engineering, Vol. 9, No. 3, pp. 195-204, 2006.
- [7] Attia, H.A., The Effect of Variable Properties on the Unsteady Couette Flow with Heat Transfer Considering the Hall Effect, Communications in Nonlinear Science and Numerical Simulation, Vol.13, pp. 1596-1604, 2008.
- [8] Md. Ziaul Haque and Md. Mahmud Alam, Micropolar Fluid Behabiours on Unsteady MHD Heat and Mass Transfer Flow with Constant Heat and Mass fluxes, Joule Heating and Viscous Dissipation, AMSE Journal, Vol. 80, No. 1-2, 2011.
- [9] Krishnendu Bhattacharyya, MHD Stagnation-point Flow of Casson fluid and Heat Transfer over a Stretching Sheet with the Thermal Radiation”, Journall of Thermodynamics, Article ID 169674, pp. 1-9, 2013.
- [10] Md. Faisal Kabir and Md. Mahmud Alam, Unsteady Casson Fluid Flow through a Parallel Plate with Hall Current, Joule Heating and Viscous Dissipation, AMSE Journal, Paper No. 14031 (2B), 2015 (Accepted).